

## EVIDENCE FOR RESONANCES IN THE $7\alpha$ DISASSEMBLY OF $^{28}\text{Si}^*$

X.G. CAO<sup>a,b</sup>, E.J. KIM<sup>b,c</sup>, K. SCHMIDT<sup>b,d</sup>, J.B. NATOWITZ<sup>b</sup>  
K. HAGEL<sup>b</sup>, M. BARBUI<sup>b</sup>, J. GAUTHIER<sup>b</sup>, S. WUENSCHL<sup>b</sup>, R. WADA<sup>b</sup>  
N. BLANDO<sup>b</sup>, G. GIULIANI<sup>e</sup>, H. ZHENG<sup>e</sup>, A. BONASERA<sup>e</sup>  
M.R.D. RODRIGUEZ<sup>b,f</sup>, S. KOWALSKI<sup>d</sup>, M. HUANG<sup>b,g</sup>, G.Q. ZHANG<sup>a</sup>  
C.Y. WONG<sup>h</sup>, A. STASZCZAK<sup>i</sup>, Z.X. REN<sup>j</sup>, Y.K. WANG<sup>j</sup>, S.Q. ZHANG<sup>j</sup>  
J. MENG<sup>j,k</sup>

<sup>a</sup>Shanghai Institute of Applied Physics, Chinese Academy of Sciences  
Shanghai 201800, China

<sup>b</sup>Cyclotron Institute, Texas A&M University, College Station, Texas 77843, USA

<sup>c</sup>Division of Science Education, Chonbuk National University  
567 Baekje-daero Deokjin-gu, Jeonju 54896, Korea

<sup>d</sup>Institute of Physics, University of Silesia, 40-007 Katowice, Poland

<sup>e</sup>Laboratori Nazionali del Sud, INFN, via Santa Sofia, 62, 95123 Catania, Italy

<sup>f</sup>Instituto de Física, Universidade de São Paulo

Caixa Postal 66318, CEP 05389-970, São Paulo, SP, Brazil

<sup>g</sup>College of Physics and Electronics Information

Inner Mongolia University for Nationalities, Tongliao, 028000, China

<sup>h</sup>Physics Division, Oak Ridge National Laboratory, Oak Ridge, USA

<sup>i</sup>Institute of Physics, Maria Curie-Skłodowska University, 20-031 Lublin, Poland

<sup>j</sup>State Key Laboratory of Nuclear Physics and Technology, School of Physics  
Peking University, Beijing 100871, China

<sup>k</sup>Yukawa Institute for Theoretical Physics, Kyoto University  
Kyoto 606-8502, Japan

*(Received January 8, 2019)*

Observations of resonance structures in the excitation function of the  $7\alpha$  de-excitation of  $^{28}\text{Si}$  nuclei in the collisions of 35 MeV/nucleon  $^{28}\text{Si}$  with  $^{12}\text{C}$  may indicate that toroidal high-spin isomers such as those predicted by recent theoretical calculations are populated.

DOI:10.5506/APhysPolBSupp.12.307

---

\* Presented at the XIII Workshop on Particle Correlations and Femtoscopy, Kraków, Poland, May 22–26, 2018.

## 1. Introduction

The existence of exotic shapes for nuclei with high excitation energy and/or angular momentum has been predicted for a long time [1]. Pursuing this suggestion, Wong studied possible toroidal and bubble nuclei and predicted excited toroidal states in the mass region of  $40 \leq A \leq 70$  and  $A \leq 250$  [2–4]. The probability of planar fragmentation configurations was much larger than that predicted by quantum molecular dynamics calculations in data from recent experiments searching for heavy toroidal systems [5].

These studies were extended by Wong and collaborator and they predicted that toroidal configurations were also possible for nuclei with angular momenta [6–8] that were above a sufficient threshold. They were able to define the region of mass and angular momentum in which such configurations might be realized. Zhang *et al.* [9], Ichikawa *et al.* [10, 11] and Staszczak and Wong [12–14], have predicted the existence of toroidal isomers in light nuclei employing microscopic techniques in recent studies.

We have studied reactions of 35 MeV/nucleon  $^{28}\text{Si}$  on  $^{12}\text{C}$  at the Cyclotron Institute at Texas A&M University using the  $4\pi$  array, NIMROD-ISiS (Neutron Ion Multidetector for Reaction Oriented Dynamics with the Indiana Silicon Sphere), which consisted of 14 concentric rings covering from  $3.6^\circ$  to  $167^\circ$  in the laboratory frame [15]. In the forward rings with  $\theta_{\text{lab}} \leq 45^\circ$ , two special modules were set having two Si detectors (150 and 500  $\mu\text{m}$ ) in front of a CsI(Tl) detector (3–10 cm), referred to as super-telescopes. The other modules (called telescopes) in the forward and backward rings had one Si detector (one of 150, 300 or 500  $\mu\text{m}$ ) followed by a CsI(Tl) detector. The pulse shape discrimination method was employed to identify the light charged particles with  $Z \leq 3$  in the CsI(Tl) detectors. Intermediate mass fragments (IMFs) were identified with the telescopes and super-telescopes using the  $\Delta E$ – $E$  method. In the forward rings, an isotopic resolution up to  $Z = 12$  and an elemental identification up to  $Z = 20$  were achieved. We report in these proceedings a summary of a study that is described in more detail in [20].

## 2. Analysis

We focus on the  $7\alpha$  decay channels of excited projectile-like fragments produced in the reaction 35 MeV/nucleon  $^{28}\text{Si} + ^{12}\text{C}$ . The available energy in the center of mass of this system is 294 MeV and the maximum angular momentum,  $L_{\text{max}}$ , is  $94\hbar$  (a reaction cross section of 2417 mb),  $L_{\text{crit}}$  for fusion is  $26\hbar$  and the rotating liquid drop limiting angular momentum is  $40\hbar$  [16]. Initial binary configurations of excited projectile-like and target-like nuclei account for most of the reaction cross section as observed for similar collisions in this energy region [17, 18].

The excitation energy distributions of alpha-conjugate exit channels are shown in figure 1. These excitation energies are determined using calorimetric techniques where the reaction  $Q$ -value is subtracted from the sum of the kinetic energies of emitted particles in the frame of the reconstructed projectile-like nucleus

$$E_x = \sum_{i=1}^{M_{\text{cp}}} K_{\text{cp}}(i) + M_n \langle K_n \rangle - Q, \quad (1)$$

where  $M_{\text{cp}}$  is the multiplicity of charged particles,  $K_{\text{cp}}$  is the kinetic energy of a charged particle in the source frame,  $M_n$  is the neutron multiplicity,  $\langle K_n \rangle$  is the average neutron kinetic energy in the source frame and  $Q$  is the  $Q$ -value. The  $Q$ -value is zero for the  $7\alpha$  system. Results from the phenomenological event generator, HIPSE [19] as well as the AMD transport model [21] with the GEMINI [22] afterburner are also shown in the figure. The results of the AMD and HIPSE calculations are generally in good agreement with the data. The experimental  $7\alpha$  distribution, however, differs considerably from the results of the model calculations as those distributions appear to have structure at higher excitation energies.

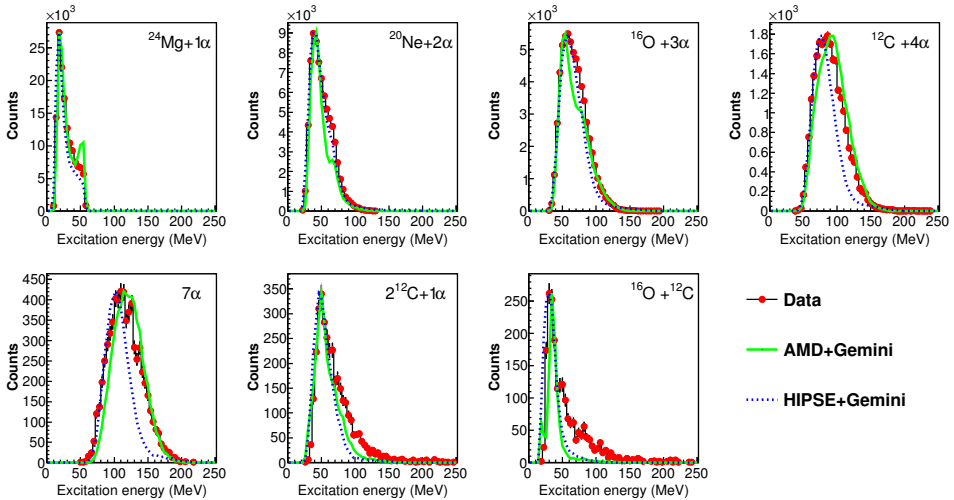


Fig. 1. Alpha-conjugate exit channel excitation functions in the de-excitation of  $^{28}\text{Si}$ . The shapes of the experimental data are compared with results of both AMD and HIPSE calculations.

The statistical code GEMINI was used to study light particle emission in detail in Ref. [23]. We have used the default parameters derived from that careful exploration [23] of the formulations of barriers and transmission coefficients, the level density and the yrast line. Events from the AMD–GEMINI [21–23] and HIPSE–GEMINI [19, 22, 23] codes were filtered

through the NIMROD acceptance. The resultant distributions were normalized to the data that are also shown in the figure. These models are not expected to produce high-energy resonances.

The experimental  $7\alpha$  distribution shown in figure 1 spans the energy region in which toroidal configurations are predicted [12] and the stablized 143.18 MeV state is predicted to exist. A maximum in the distribution is observed at  $\sim 110$  MeV and shows some structure at 126 and 138 MeV. The structure is somewhat broad due to the granularity and angular resolution of NIMROD-ISiS. This means that NIMROD-ISiS is not optimal for searches of resonances that may be very narrow since the transformation to the source frame relies on the angle of detection that has significant uncertainty. An experimental filter shows that a narrow resonance filtered through the acceptance of the detector results in a peak that has a standard deviation,  $\sigma$ , of  $\sim 4$  MeV because of the angular uncertainty. The widths of the structures observed are, therefore, consistent with much narrower resonances in the excitation energy distribution.

The experimental  $7\alpha$  distribution is compared to an uncorrelated  $7\alpha$  spectrum in the left-hand side of figure 2. This uncorrelated spectrum is constructed to represent the  $7\alpha$  phase-space in the excitation energy region. Contributions from all possible combinations of  $\alpha$ -particle emission that lead to  $7\alpha$  events regardless of the source that they might originate from are included in this uncorrelated background. The right-hand side of figure 2 shows the distribution resulting from the uncorrelated spectrum subtracted from the experimental  $7\alpha$  distribution. Prominent peaks are observed at 126 and 138 MeV and there is, in addition, some excess observed at 114 MeV. The AMD-GEMINI simulation can also be used to estimate the background. The experimental distribution with the AMD-GEMINI distribution subtracted is also shown in the right-hand side of figure 2. Both subtracted distributions show similar structures. We have performed a statistical analysis and the statistical significance peak at 114 MeV is  $5.3\sigma$ , at 126 MeV is  $8.0\sigma$  and at 138 MeV is  $7.2\sigma$  [24].

The angular momenta associated with the observed peaks would be an important ingredient in understanding whether these peaks result from toroidal configurations. If the state observed at 138 MeV, indeed, corresponds to the predicted 143.18 MeV toroidal state, the angular momentum would be  $44\hbar$ . The AMD and HIPSE models which use semi-classical techniques do not have the necessary ingredients to explore such detailed structure at these high excitation energies and angular momenta, but calculations using these models indicate that angular momenta in the range of  $40\hbar$  are reached. Our experiment, unfortunately, does not give direct information on the angular momentum.

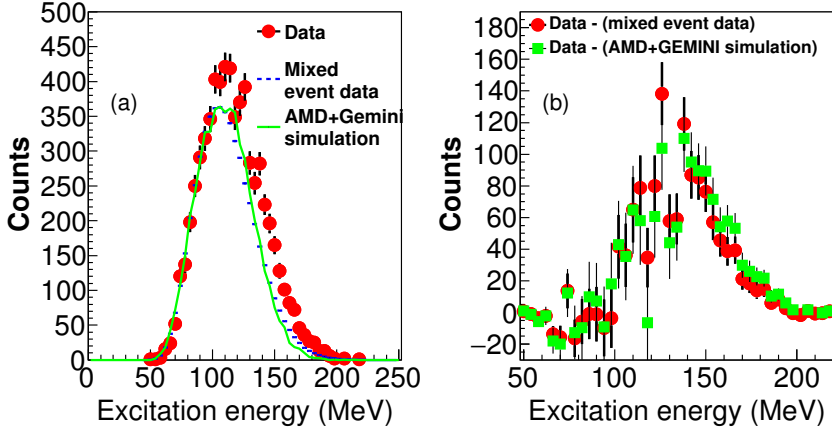


Fig. 2. Excitation energy distribution leading to observed  $7\alpha$  events. (a) The data are represented by the solid points. An uncorrelated spectrum derived from event mixing is represented by a long-dashed line. The filtered result from an AMD–GEMINI calculation is indicated by the dot-dashed line (see the text). The last two are normalized to the experimental spectrum at the lower edge of the spectrum. (b) The differences between the experimental spectrum and the others are presented.

### 3. Comparison with models

#### 3.1. Toroidal Shell Model

Resonances at the observed high excitation energies observed in the  $7\alpha$  channel are rather unusual. We have explored whether a model in which nucleons move in a toroidal potential  $V(\rho, z) = \frac{1}{2}m\omega_0^2(\rho - R)^2 + \frac{1}{2}m\omega_0^2z^2$  [2, 3, 12] may describe these resonances. Calculations using this model yield the spin and relative energy for various  $^{28}\text{Si}^*$  toroidal high-spin isomer states. The results of these calculations are shown in Table I.

Table I shows that the toroidal shell model predicts 10 toroidal high-spin isomer states up to  $4p-4h$  excitations. The predicted excitation energies are in the range of excitation energies that are shown in the experimental data in Fig. 1. These results indicate that a spinning toroidal  $^{28}\text{Si}^*$  appears as a set of toroidal high-spin isomer states with energies shown in column 3 of Table I. The excitation energy spectrum shows a number of features of toroidal signatures, *e.g.* sharp resonances at appropriate energies, spacings between a number of the resonances and the apparent presence of isomer states at excitation energies higher than the predicted  $I = 44\hbar$  state. These quantities show significant overlap with the experimental data and provide evidence of possible production of toroidal high-spin isomers in this experiment.

TABLE I

Toroidal high-spin isomers (THSI) of  $^{28}\text{Si}^*$  in the toroidal shell model. The spin-aligning ( $n$  particle)–( $n$  hole) excitations for neutrons ( $\nu$ ) and protons ( $\pi$ ), relative to a toroidal core with  $I = 0$  and energy  $E_0$ , lead to the THSI state of spin  $I = I_z$ , and excitation energy  $E_I$ .

Configurations	$I$	$(E_I - E_0)$ in $\hbar^2/2mR^2$	$E_I$ [MeV]
$(0p-0h)_\nu(0p-0h)_\pi$	0	0	91.82
$(1p-1h)_\nu(1p-1h)_\pi$	16	14	101.2
$(0p-0h)_\nu(2p-2h)_\pi + (2p-2h)_\nu(0p-0h)_\pi$	14	14	101.2
$(2p-2h)_\nu(2p-2h)_\pi$	28	28	110.58
$(2p-2h)_\nu(3p-3h)_\pi + (3p-3h)_\nu(2p-2h)_\pi$	36	49	124.65
$(3p-3h)_\nu(3p-3h)_\pi$	44	70	138.72
$(3p-3h)_\nu(4p-4h)_\pi + (4p-4h)_\nu(3p-3h)_\pi$	50	91	152.79
$(4p-4h)_\nu(4p-4h)_\pi$	56	112	166.86

### 3.2. Relativistic mean-field CDFT theory

Covariant density functional theory (CDFT) [25] which exploits symmetries and the separation of scales and, in general, the basic properties of QCD at low energies can also be used to search for toroidal isomer states. The CDFT theory has proven to be an excellent description of ground and excited states with high predictive power for nuclei throughout the periodic table [26–28]. It provides significant confidence in the investigation of nuclear toroidal structures without assuming the existence of clusters *a priori* when using a universal density functional.

We have employed the cranking CDFT in 3D lattice space [29, 30] to investigate toroidal states in  $^{28}\text{Si}$  using the density functionals, PC-PK1 [31] and DD-ME2 [32]. The  $z$  axis is chosen as the symmetry axis, and grid points  $34 \times 34 \times 24$  are chosen for  $x$ ,  $y$  and  $z$ , respectively. Self-consistency is assured by requiring an accuracy of  $10^{-4}$  MeV for single-particle levels.

Toroidal states with  $I = 0\hbar, 14\hbar, 16\hbar, 28\hbar, 36\hbar, 44\hbar, 50\hbar, 56\hbar$  have been identified corresponding to excitation energies of 72, 91, 89, 106, 128, 148, 168, and 185 MeV, respectively, using the covariant functional PC-PK1 [31] in the CDFT formalism. The same angular momentum states with the same configurations were also identified with similar excitation energies using the covariant functional DD-ME2[32].

The stability of the toroidal isomers against particle emission has been investigated by examining the radial density distributions of occupied single-particle levels as well as the total density distributions of the predicted toroidal states. Neutron densities in the predicted toroidal state with

$I = 28\hbar$  are shown in figure 3. The figure shows that the radial density distributions are, in fact, localized for all predicted toroidal states indicating that the predicted toroidal isomer states are stable against particle emission.

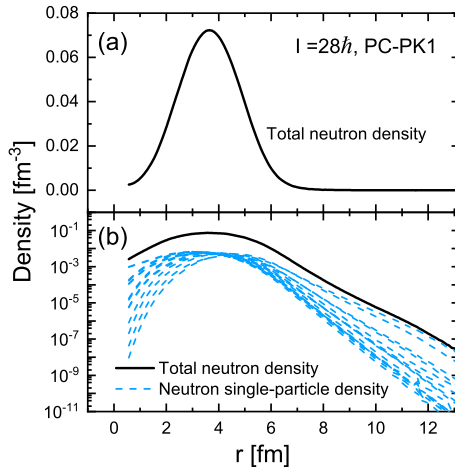


Fig. 3. (Color online) Neutron radial density distributions ( $z$  direction is integrated) of the occupied single-particle levels (blue, thin lines) as well as the total density distribution (black, thick lines) in toroidal state with  $I = 28\hbar$ .

It should be noted that all toroidal high-spin isomer states predicted by the previous theoretical result have been identified in the relativistic mean-field CDFT theory. This supports the use of the toroidal shell model as the signature for toroidal high-spin isomers.

#### 4. Summary and conclusions

We have observed that the excitation function of the  $7\alpha$  decay channel of 35 MeV/nucleon  $^{28}\text{Si} + ^{12}\text{C}$  reveals structure at high excitation energies. These structures are observed at excitation energies that are similar to those predicted by several theoretical calculations in which toroidal shell effects stabilize the nucleus against major radius variations while spin aligning particle-hole expectations lead to many high-spin toroidal isomers. We note that recent work indicates that clustering effects are important in the collisions of alpha-conjugate nuclei [33, 34]. Further experimental work is clearly necessary. A position-sensitive detector system with high granularity and the addition of gamma-ray detectors could provide significant improvement to allow more definite conclusions.

This work was supported by the United States Department of Energy under grants Nos. DE-FG03-93ER40773 and DE-AC05-00OR22725 with UT-Battelle, LLC (Oak Ridge National Laboratory) and by The Robert A. Welch Foundation under grant No. A0330. Partial support by the National Natural Science Foundation of China under contracts Nos. 11421505, 11335002, 11621131001, and 11305239 and the Youth Innovation Promotion Association CAS (No. 2017309) are acknowledged. Travel support for C.Y. Wong under the CUSTIPEN Program is thankfully acknowledged. We appreciate useful communications from A. Ono, J. Maruhn, T. Ichikawa and S. Umar. We also greatly appreciate the efforts of the staff of the TAMU Cyclotron Institute.

## REFERENCES

- [1] J.A. Wheeler, Nucleonics Notebook, 1950 (unpublished), see also p. 297 in G. Gamow, *Biography of Physics*, Harper & Brothers Publishers, N.Y. 1961; Princeton University Graduate Course Physics 576 Take-Home Examination Problem 2, May 22, 1963 (unpublished).
- [2] C.Y. Wong, *Phys. Lett. B* **41**, 446 (1972).
- [3] C.Y. Wong, *Ann. Phys. (NY)* **77**, 279 (1973).
- [4] C.Y. Wong, in: *Superheavy Elements*, (ed.) M.A.K. Lodhi, Pergamon Press, New York 1978, p. 524.
- [5] R. Najman *et al.*, *Phys. Rev. C* **92**, 064614 (2015).
- [6] C.Y. Wong, *Phys. Rev. C* **17**, 331 (1978).
- [7] C.Y. Wong, *Phys. Rev. Lett.* **55**, 1973 (1985).
- [8] J.Y. Zhang, C.Y. Wong, *Phys. Rev. C* **34**, 1094 (1986).
- [9] W. Zhang, H.Z. Liang, S.Q. Zhang, J. Meng, *Chin. Phys. Lett.* **27**, 102103 (2010).
- [10] T. Ichikawa *et al.*, *Phys. Rev. Lett.* **109**, 232503 (2012).
- [11] T. Ichikawa, K. Matsuyanagi, J.A. Maruhn, N. Itagaki, *Phys. Rev. C* **89**, 011305 (2014); **90**, 034314 (2014).
- [12] A. Staszczak, C.Y. Wong, *Phys. Lett. B* **738**, 401 (2014).
- [13] A. Staszczak, C.Y. Wong, *Acta Phys. Pol. B* **46**, 675 (2015).
- [14] A. Staszczak, C.Y. Wong, *Phys. Scr.* **90**, 114006 (2015).
- [15] S. Wuenschel *et al.*, *Nucl. Instrum. Methods Phys. Res. A* **604**, 578 (2009).
- [16] W.W. Wilcke *et al.*, *At. Data Nucl. Data Tables* **25**, 389 (1980).
- [17] K. Hagel *et al.*, *Phys. Rev. C* **50**, 2017 (1994).
- [18] Y. Larochelle *et al.*, *Phys. Rev. C* **53**, 823 (1996).
- [19] D. Lacroix, A. Van Lauwe, D. Durand, *Phys. Rev. C* **69**, 054604 (2004).
- [20] X.G. Cao *et al.*, *Phys. Rev. C* **99**, 014606 (2019) [arXiv:1801.07366 [nucl-ex]].

- [21] A. Ono, *Phys. Rev. C* **59**, 853 (1999).
- [22] R.J. Charity, *Phys. Rev. C* **82**, 014610 (2010).
- [23] D. Mancusi, R.J. Charity, J. Cugnon, *Phys. Rev. C* **82**, 044610 (2010).
- [24] S.I. Bityukov, N.V. Krasnikov, [arXiv:physics.data-an/9809037](https://arxiv.org/abs/physics.data-an/9809037).
- [25] J. Meng, (ed.), *Relativistic Density Functional for Nuclear Structure*, International Review of Nuclear Physics, Vol. 10, World Scientific, Singapore 2016.
- [26] J. Meng, J. Peng, S.Q. Zhang, P.W. Zhao, *Front. Phys.* **8**, 55 (2013).
- [27] J. Meng *et al.*, *Prog. Part. Nucl. Phys.* **57**, 470 (2006).
- [28] H.Z. Liang, J. Meng, S.-G. Zhou, *Phys. Rep.* **570**, 1 (2015).
- [29] Z.X. Ren, S.Q. Zhang, J. Meng, *Phys. Rev. C* **95**, 024313 (2017).
- [30] Z.X. Ren *et al.*, to be published.
- [31] P.W. Zhao, Z.P. Li, J.M. Yao, J. Meng, *Phys. Rev. C* **82**, 054319 (2010).
- [32] G.A. Lalazissis, T. Nikšić, D. Vretenar, P. Ring, *Phys. Rev. C* **71**, 024312 (2005).
- [33] K. Schmidt *et al.*, *Phys. Rev. C* **95**, 054618 (2017).
- [34] B. Schuetrumpf, W. Nazarewicz, *Phys. Rev. C* **96**, 064608 (2017).